BULLETIN

of the

American Meteorological Society

Assistant Editor
THOMAS A. GLEESON
Florida State University
Tallahassee, Florida

Editor
WERNER A. BAUM
Florida State University
Tallahassee, Florida

Technical Editor
JAMES S. SANDBERG
American Meteorological Society
Boston 8, Massachusetts

VOL. 42 DECEMBER, 1961 No. 12

The Divergence Equation as Related to Severe Thunderstorm Forecasting

D. C. HOUSE

U. S. Weather Bureau, Kansas City, Missouri

(Original manuscript received 17 March 1961; revised manuscript received 25 May 1961)

ABSTRACT

The divergence form of the equations of motion is developed and the terms of the equation are related to several local thunderstorm forecast parameters. It is found that the divergence equation provides the physical basis for evaluating the validity of several forecast rules under differing synoptic situations. In order that the magnitudes of the several terms can be compared, a numerical solution for a particular severe local thunderstorm producing synoptic situation is shown.

1. Introduction

Procedures and techniques [1, 2] in use today for the prediction of severe thunderstorms and tornadoes are weighted heavily towards the detection or prediction of favorable vertical motion fields. Ideally, the prediction techniques demand a knowledge of the vertical distribution of horizontal velocity divergence and the change of this distribution with time. Since the magnitude of horizontal velocity divergence is exceedingly difficult to measure with accuracy, and its rate of change is even more difficult to ascertain, the forecast procedures have been designed primarily to detect the sign of the horizontal velocity divergence and its time rate of change.

The forecaster's ability to accomplish the foregoing has been enhanced by experience and the development of forecast rules and procedures that have led to some considerable success while circumventing the basic problem of accomplishing actual measurements. In [1], parameters important to the formulation of the forecast are listed. Of these, it should be noted that the low level wind field, the jet stream and the 700-mb temperature pattern are of considerable importance to the prediction of severe local storms. In [3], Lee and Galway correlated occurrences of tornadoes with the −60C isotherm at the 200-mb level and the jet stream. Until this writing, no attempt has been made by the severe storm forecasters to relate the parameters to the time rate of change of divergence.

Since the problem of divergence production or time rate of change of divergence is so intimately related to the severe thunderstorm forecast problems, it becomes the purpose of this paper to show the physical processes involved and relate them to features that can be recognized on the synoptic weather maps through a depth of the atmosphere.

2. Formulation of the diagnostic equations

Upon ignoring friction and the small terms involving the earth's curvature, the first two equa-

Published monthly at Prince and Lemon Streets, Lancaster, Pa. Second-class postage paid at Lancaster, Pa. Address all business communications, purchase orders and inquiries regarding the Society to the *Executive Secretary, 45 Beacon Street, Boston 8, Mass.*

tions of motion can be written in the following manner:

$$\frac{du}{dt} = f(v - v_g)$$

$$\frac{dv}{dt} = -f(u - u_g),$$

where u and v are the horizontal components of the wind, f is coriolis Parameter and subscript g refers to geostrophic wind. Upon differentiating the first partially with respect to x and the second with respect y, adding the resulting equations and manipulating the terms in the result, the divergence equation (see for example [7]) can be written as:

$$\frac{d}{dt}\operatorname{div}_2 \boldsymbol{V} = f\zeta' + 2J(u, v) - (\operatorname{div}_2 \boldsymbol{V})^2 - \frac{\partial w}{\partial x}\frac{\partial u}{\partial z} - \frac{\partial w}{\partial y}\frac{\partial v}{\partial z} - \beta u' \quad (1)$$

where, $\zeta' = \zeta - \zeta_g$, $u' = u - u_g$ and $J(u, v) = (\partial u/\partial x)(\partial v/\partial y) - (\partial u/\partial y)(\partial v/\partial x)$ while β is the latitudinal variation in the Coriolis parameter, ζ is vertical component of the relative vorticity.

When above equation is applied at levels where vertical velocities are negligibly small (*i.e.*, sea level or at and in the vicinity of the jet stream) and when the term involving β is ignored, the divergence equation for horizontal frictionless flow becomes

$$\frac{d}{dt}(\operatorname{div}_2 \boldsymbol{V}) = f\zeta' + 2J(u, v) - (\operatorname{div}_2 \boldsymbol{V})^2. \quad (2)$$

Since the diagnostic and prognostic problem is to relate divergence and divergence changes through a depth of the atmosphere to synoptic features, what is required is an expression for divergence production that details the physical processes through such a depth. Such an expression can be derived by assuming that the atmosphere can be described by a divergence distribution such that one or more levels of nondivergence exist and that the first of these levels above the surface of the earth is a quasi-horizontal surface and is geostrophic. Eq (2) applied to the 1000-mb level can be written as

$$\frac{d}{dt}(\operatorname{div}_2 \boldsymbol{V})_0 = f\zeta_0' + 2J(u, v)_0 - (\operatorname{div}_2 \boldsymbol{V})_0^2 \quad (3)$$

where subscript 0 refers to 1000 mb. Since $\zeta' = \zeta - \zeta_g$ and noting that $Z_0 = Z_L - h$ (where subscript L refers to the level of nondivergence and h is thickness between 1000 mb and the level of nondivergence) we may write

$$f\zeta_0' = f\zeta_0 - f\zeta g_0 = f\zeta_0 - g\nabla^2 Z_0$$

or

$$f\zeta_0' = f\zeta_0 - g\nabla^2 Z_L + g\nabla^2 h.$$

But it was assumed that at the level of nondivergence the wind is geostrophic so that

$$g\nabla^2 Z_L = f\zeta_{gL} = f\zeta_L,$$

thus

$$f\zeta_0' = f\zeta_0 - f\zeta_L + g\nabla^2 h.$$

With substitution of the above into (3), it can be seen that

$$\frac{d}{dt}(\operatorname{div}_2 \boldsymbol{V})_0 = -f\zeta_L + f\zeta_0 + g\nabla^2 h + 2J(u, v)_0 - (\operatorname{div}_2 \boldsymbol{V})_0^2. \quad (4)$$

A similar expression can be derived for the layer from the level of nondivergence to the first level of maximum divergence above. This works out to be

$$\frac{d}{dt}(\operatorname{div}_2 \boldsymbol{V})_m = -f\zeta_L + f\zeta_m - g\nabla^2 h + 2J(u, v)_m - (\operatorname{div}_2 \boldsymbol{V})_m^2, \quad (5)$$

where subscript m refers to level of maximum divergence and h is thickness of this layer.

The terms of eq (3) are interrelated and should not be considered as separate physical processes. Likewise the terms of eq (4) and (5) are interrelated. Real practical difficulties arise in the evaluation of the equations because of the paucity of the upper air data. However, the determination of the relative importance of each term for a given synoptic situation should provide useful information for diagnostic and prognostic purposes as well as to indicate the application and validity of forecast rules that have been previously empirically derived or gained from experience.

3. Discussion of the terms

Considering first, the Jacobian term $[2J(u,v)]$ it can be seen that this term will be zero when either u or v is constant or zero.

Under initial conditions of nondivergent and geostrophic flow, the term operates to produce positive or negative divergence. The term also operates to produce additional divergence or destroy existing divergence in an initial divergent flow since it can have either a positive or negative sign.

Regardless of the sign of divergence of the real wind, the divergence squared term operates to destroy divergence. Conversely, it acts to increase convergence in existing convergent flow.

The deviation ($f\zeta'$) term is generally of the same order of magnitude as the other terms when broad scale flow patterns are considered. However, in the subsynoptic or meso scale this term is often an order of magnitude larger than the other terms. (See for example tables 1, 2 and 3.) For this reason its contribution is perhaps the easiest of three terms to deduce from synoptic data. The deviation of the real wind from the geostrophic on any given surface synoptic chart can usually be detected by careful analysis of the wind and pressure data.

Since the magnitude of the deviation term is dependent upon the difference between the vorticity of the real wind and the geostrophic vorticity, the sign of the term can frequently be deter-

TABLE 1. Computed values of terms in eq (10) at numbered grid points of fig. 1 from 0600C 4 May 1960 data. Units are multiplied by 10^{-2} hr^{-2}.

Grid point	$f\zeta$	$-f\zeta_g$	$-V\cdot\nabla(\mathrm{div}_2 V)$	$-(\mathrm{div}_2 V)^2$	$2J(u,v)$	$\frac{\partial}{\partial t}(\mathrm{div}_2 V)$
1	4.3	−9.4	+0.3	−0.1	−0.4	−5.3
2	3.0	−2.9	−1.2	−3.4	−0.0	−4.5
3	−1.0	−6.7	−5.6	−1.8	0.4	−15.5
4	−2.0	−8.1	−5.9	−1.6	0.0	−17.6
5	−2.5	0.0	+0.2	−0.6	−0.2	−3.1
6	−1.3	−3.3	+3.0	−0.1	+0.1	−1.6
7	2.3	−11.0	+0.6	−0.4	+0.6	−7.9
8	0.0	−13.6	+2.3	0.0	+0.7	−10.6
9	0.3	−9.8	−4.3	−0.6	+1.2	−13.2
10	−0.3	−1.1	−4.5	−0.4	+0.7	−5.7
11	−1.8	−5.2	+1.8	−0.1	+0.1	−5.2
12	−1.5	−11.2	+2.6	−2.8	−1.7	−14.6
13	0.8	−9.8	+1.9	−0.4	+0.2	−7.3
14	0.0	−12.2	−0.3	0.0	+0.8	−11.8
15	0.8	−1.8	−0.2	−0.1	+0.6	−0.7
16	0.0	+3.2	−0.2	−0.3	+1.1	+3.8
17	−1.8	−1.1	−0.2	0.0	+0.4	−2.7
18	−1.8	+2.8	−0.2	−2.5	−1.5	−3.2
19	2.5	−7.2	−3.4	0.0	−0.2	−8.3
20	1.0	−1.1	−5.9	−0.2	−0.4	−6.6
21	−0.5	+5.9	−1.6	−0.3	+0.3	+3.8
22	−1.3	+2.2	0.0	−0.4	+0.8	+1.3
23	−1.5	+5.5	0.2	−0.0	+0.1	+4.3
24	−0.3	+10.2	−0.9	−1.2	+0.0	+7.8
25	4.3	−2.0	−0.5	−0.7	−1.2	−1.1
26	3.5	+2.2	−1.7	−2.8	−2.1	−0.9
27	1.0	+4.8	−6.7	−1.0	−0.2	+3.9
28	0.5	+4.9	−0.0	−0.3	+0.3	+5.4
29	−0.5	+7.3	−0.5	0.0	+0.3	+6.6
30	0.3	+8.6	−0.8	−0.7	0.0	+7.4
31	3.0	−3.6	+4.6	−0.1	+0.2	+4.1
32	3.8	−2.4	+5.1	−1.6	−0.8	+4.1
33	0.8	+0.8	+2.6	−0.8	+0.4	+3.8
34	0.3	+4.4	0.0	−0.4	+0.5	+4.8
35	0.5	+4.0	−0.3	0.0	+0.1	+4.6
36	−0.3	+1.5	+2.2	−0.3	−0.1	+3.0
37	−0.3	−3.3	+3.8	−0.8	+0.6	0.0
38	−1.5	−3.3	+5.3	−0.7	−0.1	−0.3
39	−1.3	+0.9	+2.7	−0.2	+1.1	+3.3
40	0.0	+4.6	+1.7	−0.3	+1.1	+7.1
41	0.3	+0.9	+0.8	0.0	+0.4	+2.4
42	−0.8	+0.7	0.0	−0.1	−0.1	−0.3

TABLE 2. Computed values of terms in eq (10) at numbered grid points of fig. 1 from 1200C 4 May 1960 data. Units are multiplied by 10^{-2} hr^{-2}.

Grid point	$f\zeta$	$-f\zeta_g$	$-V\cdot\nabla(\mathrm{div}_2 V)$	$-(\mathrm{div}_2 V)^2$	$2J(u,v)$	$\frac{\partial}{\partial t}(\mathrm{div}_2 V)$
1	+2.8	−17.6	−0.5	0.0	−0.2	−15.5
2	+1.5	−11.8	0.0	−0.4	−0.4	−11.1
3	−0.2	−12.0	+1.2	−1.8	−0.9	−13.7
4	−1.2	−0.9	+1.8	−0.8	−0.3	−1.4
5	−0.8	+4.0	+1.5	−1.7	+1.6	+4.6
6	+1.8	−3.3	+0.4	0.0	+1.1	0.0
7	+3.5	−16.1	−0.4	−0.3	−0.3	−13.6
8	+2.2	−14.3	−0.2	−0.4	−0.4	−13.1
9	+0.5	−9.1	+1.0	−0.6	−0.4	−8.6
10	−0.2	−2.2	+1.7	−0.1	+0.1	−0.7
11	−0.2	+0.7	+1.4	−0.1	+1.5	+3.3
12	+0.2	+1.3	−0.3	0.0	+0.8	+2.0
13	+4.2	−12.3	+0.5	−0.2	−1.0	−8.8
14	+4.0	−12.9	+0.4	−0.6	−1.1	−10.2
15	+2.5	+4.5	+1.3	−1.0	−0.5	+6.8
16	−0.5	+4.0	−0.4	0.0	0.0	+3.3
17	−1.5	−6.2	−0.3	−0.4	0.0	−8.4
18	−3.2	−4.0	+0.6	0.0	−0.2	−6.8
19	+6.2	−9.6	+0.7	−0.3	−2.5	−5.5
20	+6.0	−3.6	+0.9	−0.3	−1.9	+1.1
21	+3.5	+4.2	0.0	−1.8	0.0	+5.9
22	−1.2	+5.4	−0.2	−0.7	+1.9	+5.2
23	−2.2	−2.5	−0.3	−0.1	−0.3	−5.4
24	−3.2	+2.2	+0.4	0.0	−0.6	−1.2
25	+5.8	−7.1	0.0	−0.1	−1.8	−3.2
26	+2.0	−3.8	+0.5	−0.3	0.0	−1.6
27	−1.2	+2.0	+0.4	−1.4	+0.7	+0.5
28	−1.5	+6.5	+0.9	−0.8	+0.6	+5.7
29	−1.8	+6.2	+0.2	0.0	−0.1	+4.5
30	−1.5	+5.6	0.0	0.0	0.0	+4.1
31	+1.2	−9.4	+0.7	−0.3	+2.0	−5.8
32	−2.2	−3.6	+1.4	−0.7	+1.9	+1.2
33	−3.0	+4.2	+1.3	−0.3	+1.2	+3.4
34	−1.2	+5.8	+0.8	−0.1	0.0	+5.3
35	−1.8	+7.1	0.0	0.0	+0.1	+5.4
36	−2.2	+3.6	−0.4	−0.1	+0.1	+1.0
37	+0.8	−8.7	+0.7	−0.1	+3.1	−4.2
38	−0.2	−5.6	+0.6	−0.3	+1.4	−4.1
39	−0.8	+0.9	+0.5	−0.3	+0.3	+0.6
40	−1.0	+4.7	+0.1	−0.1	0.0	+3.9
41	−2.2	+5.4	0.0	0.0	+0.1	+3.3
42	−2.5	+4.5	−0.2	0.0	+0.1	+1.9

mined by an inspection of these data. One combination of these vorticities that would contribute to divergence production is anticyclonic geostrophic vorticity and cyclonic vorticity in the real wind field. Conversely, convergence production occurs with cyclonic geostrophic vorticity and anticyclonic vorticity in the real wind.

As has already been indicated, the forecast problem is one of detecting and predicting the change in the vertical motion fields. Eq (4) and (5) detail the physical processes that contribute to that change through a depth of the atmosphere. Considering the first three terms of the right branch of eq (4), the equation states that for each term to contribute toward the production of convergence at 1000 mb or sea level that:

(1) Cyclonic geostrophic vorticity (*e.g.*, short wave trough) is required at the level of nondivergence.
(2) Anticyclonic vorticity in the real wind is required at 1000 mb or sea level. This specifies the role of the low-level jet.
(3) Anticyclonic thermal vorticity of the layer is required. Stated another way, the configuration of the thickness pattern must be favorable such as is the case with a thickness ridge.

The more frequent combination of these three terms in the production of convergence appears to come about from an imbalance between their contributions. For example, under conditions of favorable thickness patterns, convergence production is a result of

(1) greater cyclonic vorticity at the level of nondivergence than at sea level, or
(2) greater anticyclonic vorticity at the sea level than at the level of nondivergence.

Considering now the first three terms of the right branch of eq (5) it can be seen that what is required for each term to contribute towards divergence production at the level of maximum divergence is:

(1) Cyclonic relative vorticity (*e.g.*, a short wave trough), at the level of maximum divergence,
(2) Anticyclonic relative geostrophic vorticity at the level of nondivergence, and
(3) A ridge in the thickness pattern for the layer.

Again it is important to note that probably the most frequent combination of these three terms in the production of divergence comes about as an imbalance between their contributions.

When the atmosphere from sea level to the level of maximum divergence is considered under the assumptions made in section 2, it can be seen that for vertical motion to increase with time, divergence production must occur in the upper layer

TABLE 3. Computed values of terms in eq (10) at numbered grid points of fig. 1 from 1800C 4 May 1960 data. Units are multiplied by 10^{-2} hr^{-2}.

Grid point	$f\zeta$	$-f\zeta_g$	$-V\cdot\nabla(\mathrm{div}_2 V)$	$-(\mathrm{div}_2 V)^2$	$2J(u,v)$	$\frac{\partial}{\partial t}(\mathrm{div}_2 V)$
1	4.3	−26.5	−0.1	−0.7	−1.0	−24.0
2	3.0	−18.3	+0.2	−0.3	−0.6	−15.4
3	2.5	−3.1	−0.5	0.0	−0.3	−1.4
4	0.5	−0.5	−0.4	0.0	0.0	−0.4
5	−2.3	+0.2	−0.2	0.0	−0.1	−2.4
6	−3.0	+0.7	−0.2	−0.1	−0.6	−4.2
7	3.8	−19.2	−0.7	−0.8	−1.2	−18.1
8	2.8	−8.0	−0.5	−0.4	−0.3	−6.4
9	1.5	+14.5	−0.5	0.0	0.0	+15.5
10	−1.3	0.0	−0.2	0.0	−0.1	−1.6
11	−2.5	+1.3	+0.2	−0.1	−0.3	−1.4
12	−1.8	+8.5	−0.1	0.0	−0.3	+6.3
13	3.3	−4.2	−1.6	−1.8	−1.2	−5.5
14	2.8	+8.7	−1.8	−1.4	−0.5	+7.8
15	0.3	+8.3	−0.2	−0.1	0.0	+8.3
16	−1.3	+2.9	+0.4	−0.1	0.0	+1.9
17	−2.0	+2.9	+0.5	0.0	−0.1	+1.3
18	−0.8	+3.8	+0.2	0.0	−0.1	+3.1
19	+3.8	+4.7	−1.2	−4.7	−2.9	−0.3
20	1.8	+3.6	−2.0	−2.5	−0.6	+0.3
21	0.5	−4.0	+0.7	−0.3	−0.4	−3.5
22	−0.8	+3.8	−0.1	0.0	−0.1	+3.0
23	−1.8	−6.9	+0.2	0.0	0.0	−8.5
24	−1.5	−4.0	+0.1	0.0	0.0	+5.4
25	5.0	−7.1	+5.3	−5.1	0.0	−1.9
26	4.0	+11.6	−2.5	−2.8	+0.8	+11.1
27	3.3	+1.1	−2.6	−0.7	0.0	+1.1
28	1.3	−11.6	−0.3	0.0	−0.2	−10.8
29	−1.0	−7.1	−0.2	0.0	0.0	−8.3
30	−1.5	+1.1	0.0	0.0	−0.1	−0.5
31	3.0	−7.6	+7.1	−0.2	+1.0	+3.3
32	5.3	−9.8	+3.4	−4.7	+1.0	−4.8
33	4.5	−5.8	−2.6	−3.3	−2.1	−8.3
34	2.8	−6.9	−1.2	−0.8	−0.4	−6.5
35	−0.3	+0.7	+0.4	−0.2	0.0	+0.6
36	−0.8	+0.5	0.0	0.0	0.0	0.0
37	−2.8	−4.0	+6.8	−0.1	+1.2	+1.1
38	0.0	+0.5	+4.7	−4.3	+2.1	+3.0
39	1.3	−7.1	+1.0	−5.9	0.0	−10.7
40	0.0	−0.5	−0.5	−2.0	−0.2	−3.2
41	−0.8	+3.6	0.0	−0.3	−0.1	−3.2
42	0.0	+1.1	+0.5	0.0	+0.2	+1.8

and convergence production must occur in the lower layer. Eq (4) and (5) then can be used to specify the synoptic features that should exist. One such combination is as follows:

1. Anticyclonic relative vorticity in wind field at 1000 mb or sea level.
2. A thickness ridge through the depth of the atmosphere below the level of maximum divergence.
3. Zero relative geostrophic vorticity at the level of nondivergence, such as would be the case in uniform contour gradient without curvature.
4. Cyclonic relative vorticity in real wind field at the level of maximum divergence equal in magnitude to anticyclonic relative vorticity of real wind at 1000 mb or sea level.

4. The case of 4 May 1960

By way of illustrating the foregoing, the severe thunderstorm case of 4 May 1960 was selected for study. Since what the forecaster desires to ascertain is how divergence is changing locally, eq (3) was rewritten (ignoring vertical advection of divergence)

$$\frac{\partial}{\partial t}(\mathrm{div}_2 V) = f\zeta' + 2J(u, v) - (\mathrm{div}_2 V)^2 - V\cdot\nabla(\mathrm{div}_2 V). \quad (6)$$

Values of the terms of the right branch of (6) were secured at the numbered grid points of fig. 1 (which are 60 nm apart) as follows:

1. All computations were made using a measuring interval of 120 nm.

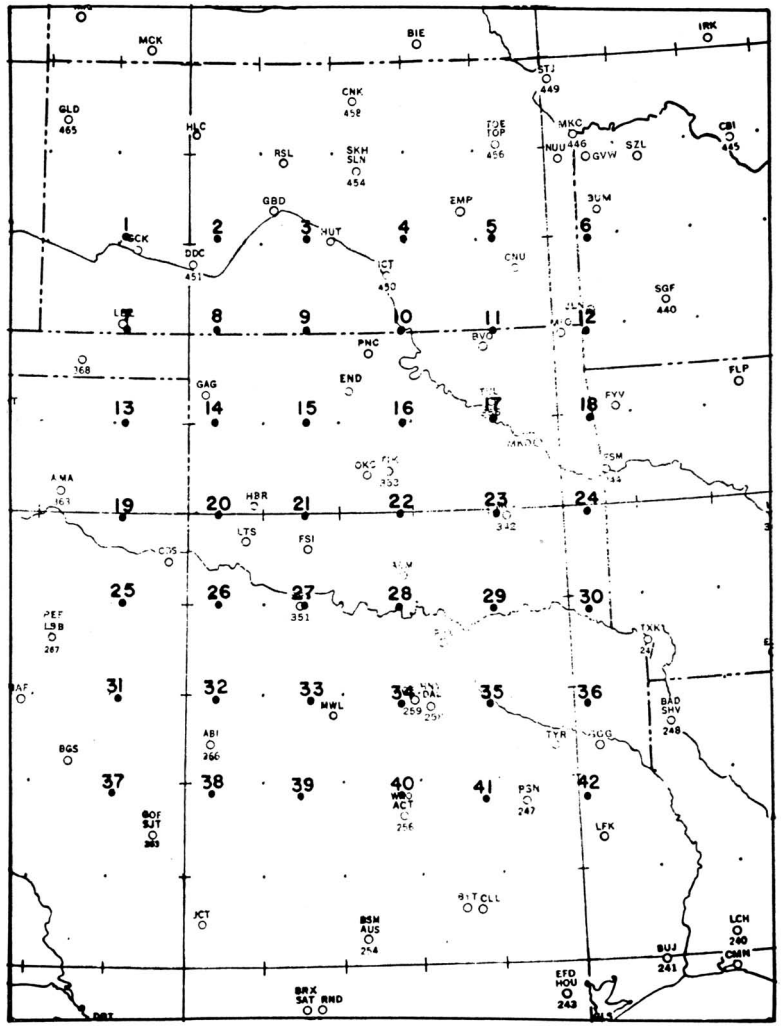

FIG. 1. Location of grid points about which computations were performed.

2. Wind observations at second standard level of the pibal were used in computations of the divergence, advection of divergence, the Jacobian term, and vorticity.
3. Surface pressure data were used to compute relative geostrophic vorticity.

The values of these quantities as ascertained at the numbered grid points are shown in tables 1, 2, and 3, at the times of 0600C, 1200C and 1800C.

The surface pressure field with the divergence values indicated thereon, the wind field, represented by streamlines and isotachs, and the local change in divergence field are shown in figs. 2a, 2b, 2c, 3a, 3b, 3c and 4a, 4b, 4c, for the times of 0600C, 1200C, and 1800C, respectively. In addition figs. 2d and 4d show the 500-mb contour field and the 1000-500-mb thickness field while figs. 2e and 4e show the 200-mb contour field and the 500-200-mb thickness field for 0600C and 1800C. Finally fig. 5 shows the distribution of severe weather that occurred during the period 1200C to midnight on 4 May.

From fig. 5 the relationship of the occurrence of severe storms to existing divergence and the local change in divergence can be ascertained.

Utilizing eq (4) and (5) for diagnostic purposes it can be seen that at 0600C (fig. 2d) for the layer 1000-500 mb a thickness ridge existed from Lubbock, Texas, northward through western Kansas. According to eq (4) this configuration would be favorable for convergence production. However, anticyclonic geostrophic vorticity at 500 mb (here 500 mb is assumed to be the level of nondivergence) and cyclonic vorticity at sea level in the same area would oppose the contribution towards convergence production of the favorable thickness configuration. Similarly a thickness ridge existed in the layer 500-200 mb from the Texas panhandle into western Kansas (fig. 2e) which according to eq (5) would contribute towards divergence production. Here the 200-mb level is considered to approximate the level of maximum divergence. Anticyclonic geostrophic vorticity at 500 mb and cyclonic vorticity of the wind field at 200 mb exist. This combination of vorticities and thickness is favorable for divergence production at the 200-mb level.

At 1800C a favorable thickness pattern for the layers sea level to 500 mb (fig. 4d) and 500-200 mb (fig. 4e) exists over western Oklahoma while the vorticities at the three levels, indicate a maximum contribution toward convergence production at sea level and divergence production at the 200-mb level over south central Oklahoma. This is borne out by the computations from eq (6), for sea level.

5. Summary

Lee and Galway [3] correlated the occurrences of tornadoes with the intersection of the jet stream and the −60C isotherm at 200-mb level. The success of this rule seems to depend upon (1) how precisely the −60C isotherm is related to a favorable thickness pattern for the layer from the level of nondivergence to the jet stream level and (2) a favorable imbalance between the vorticities at the two levels to increase divergence with time at the jet stream level.

One favorable parameter listed in [1] was the 700-mb no change advection line. The forecast success in utilizing this feature would according to the equations depend at least in part upon how adequately the 700-mb temperature field approximates the mean temperature for the layer sea level to the level of nondivergence.

Another favorable parameter listed in [1] is the existence of the low level jet. The success of the related forecast rules are dependent upon (1) the existing convergence field associated therewith, (2) the production of divergence through the Jacobian term, the divergence squared term and the deviation between the real and geostrophic vorticities, or (3), under conditions of favorable thickness patterns, the difference between the vorticities at the bottom and top of the layer.

Magar [4, 5] has described in detail meso-scale severe thunderstorm producing low pressure systems. The divergence equations shown here can be utilized to account for the rapidity by which convergence can be produced in such situations leading to the rapid onset of severe thunderstorms.

The divergence form of the equation of motion provides the link between certain empirical rules that have been utilized in severe local storm predictions and the physical processes that work toward the production or destruction of the divergence. Consequently forecast rules can be applied in the light of the physical processes deduced from synoptic weather data. The validity of forecast rules with respect to particular synoptic situations can also be established.

In essence, theoretical considerations indicate that valid forecast rules or series of rules concerning the production of divergence should be related to the decrease in anticyclonic vorticity with height or an increase of cyclonic vorticity with height. These coupled with rules concerning the favorable configuration of thickness will provide useful diag-

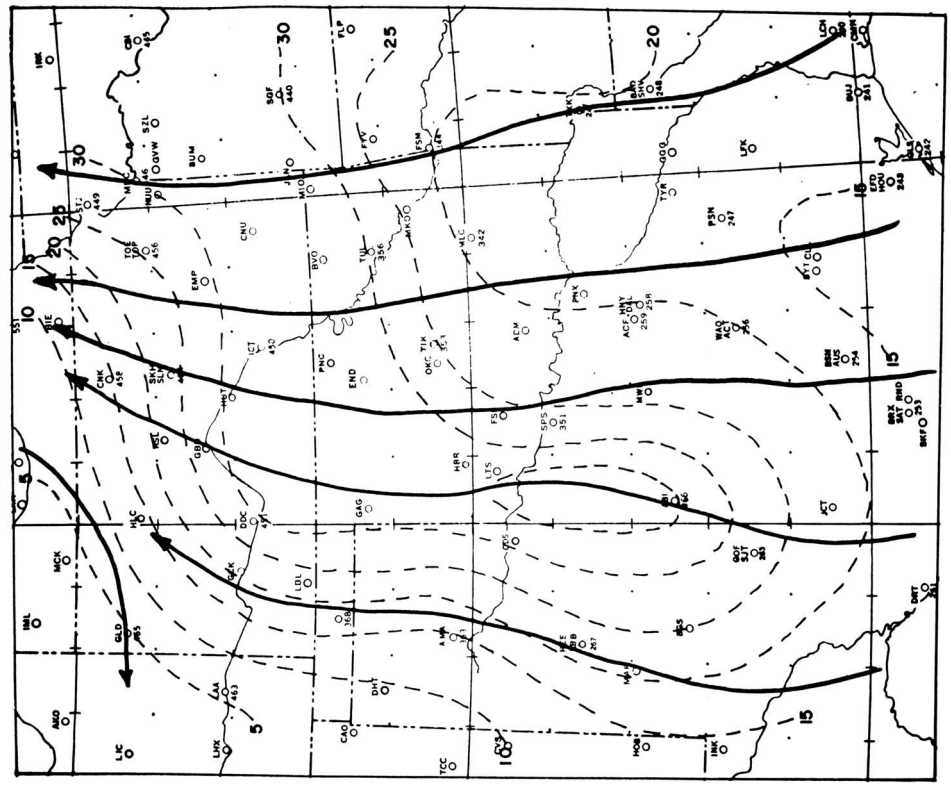

FIG. 2b. 0600C 4 May 1960 streamline and isotach analysis based upon second standard level wind observations. Isotachs are in knots.

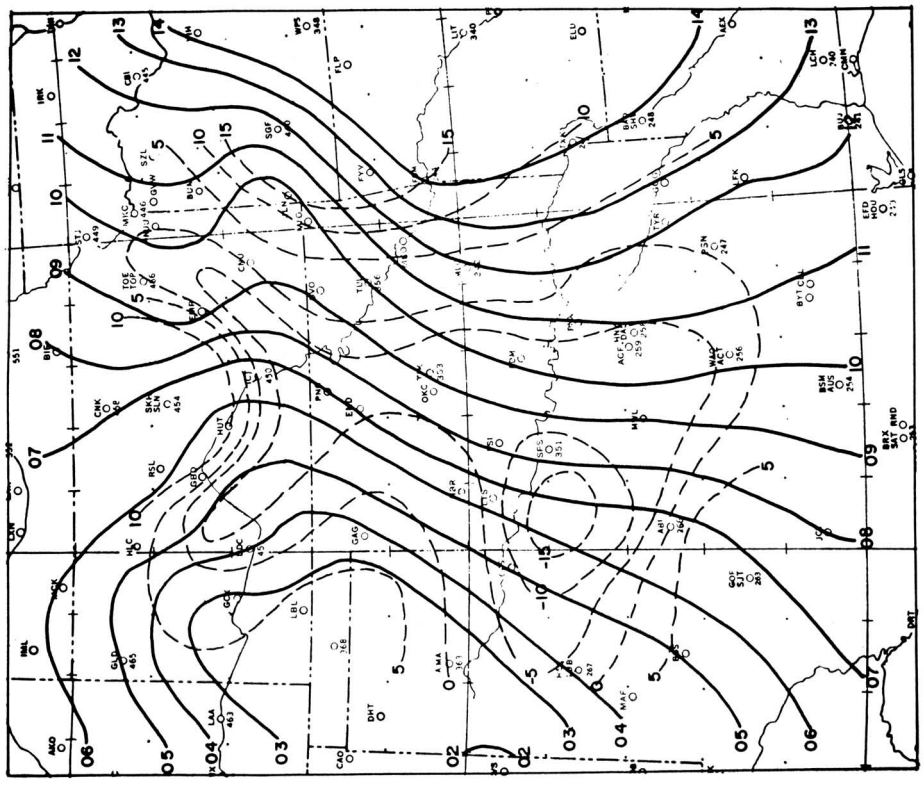

FIG. 2a. 0600C 4 May 1960 surface pressure and horizontal velocity divergence distribution. Solid lines are isobars at one-mb intervals. Dashed lines are isopleths of divergence. Units are 10^{-5} hr^{-1}. Positive values divergence, negative values convergence.

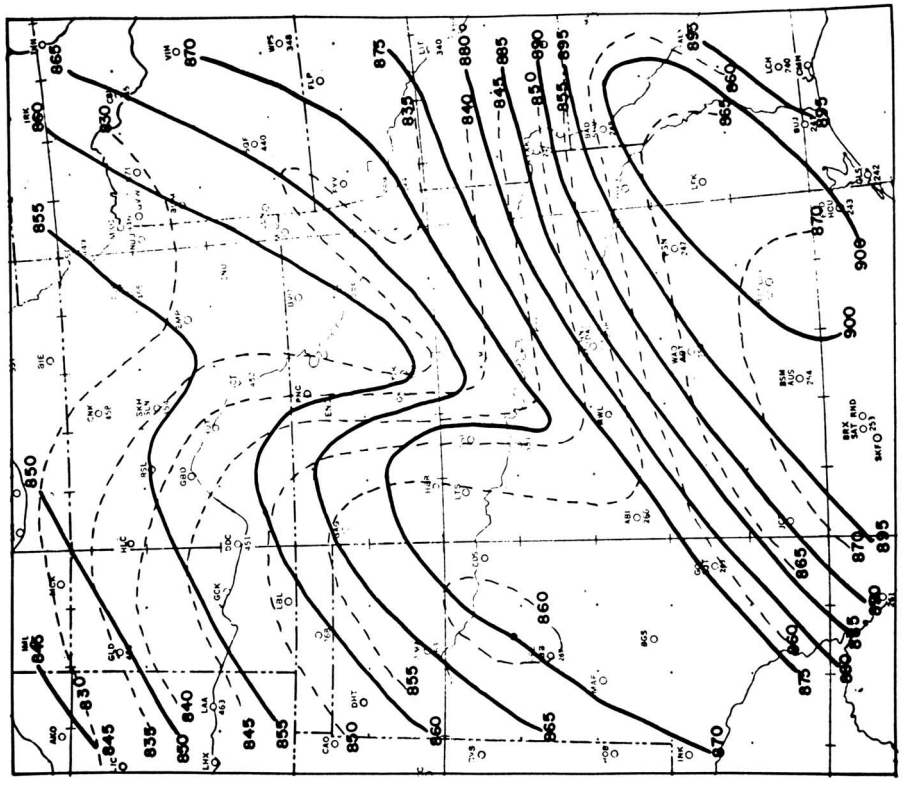

FIG. 2d. 0600C 4 May 1960, 500-mb contours and 1000–500 mb thickness contours. Solid lines are 500-mb contours; dashed lines are thickness contours. All contours are at 50-ft intervals.

FIG. 2c. Isopleths are values of $\partial/\partial t \operatorname{div}_2 V$ at 0600C, 4 May 1960. Units are 10^{-2} hr^{-2}. Negative values represent increasing convergence with time while positive values represent increasing divergence with time.

FIG. 3a. 1200C 4 May 1960 surface pressure and horizontal velocity divergence distribution. Solid lines are isobars at one-mb intervals; dashed lines are isopleths of divergence. Units are 10^{-2} hr^{-2}.

FIG. 2e. 0600C 4 May 1960, 200-mb contours and 500–200 mb thickness contours. Solid lines are 200-mb contours at 100-ft intervals; dashed lines are thickness contours at 50-ft intervals.

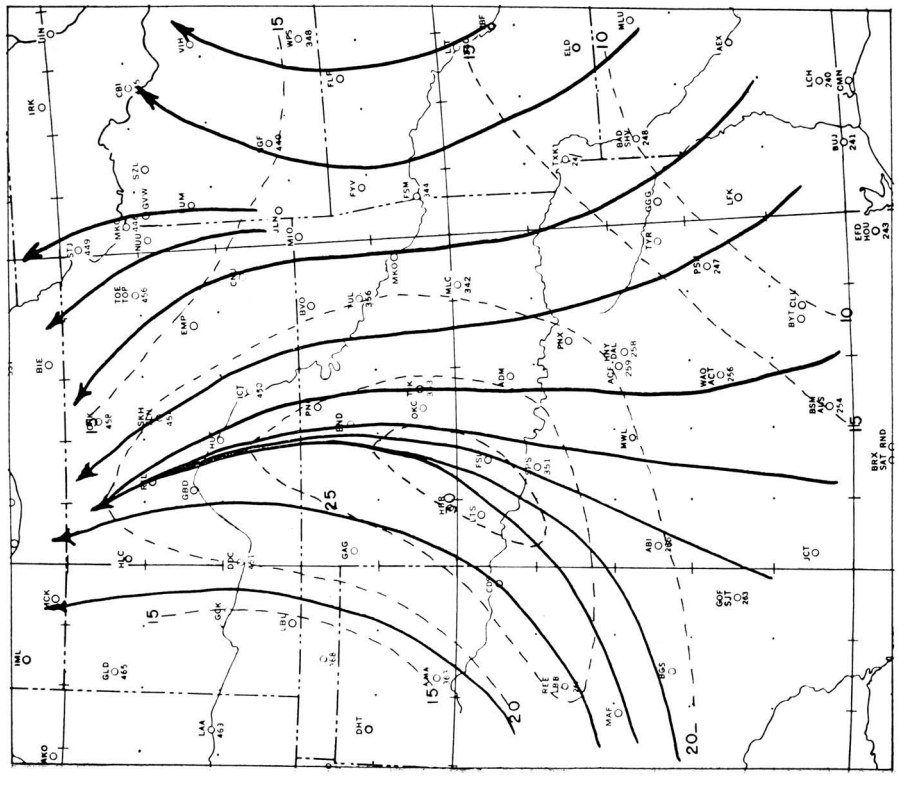

FIG. 3b. 1200C 4 May 1960 streamline and isotach analysis based upon second standard level wind observations.

FIG. 3c. Isopleths are values of $\partial/\partial t \, \mathrm{div}_2 V$ at 1200C 4 May 1960. Units are 10^{-2} hr^{-2}.

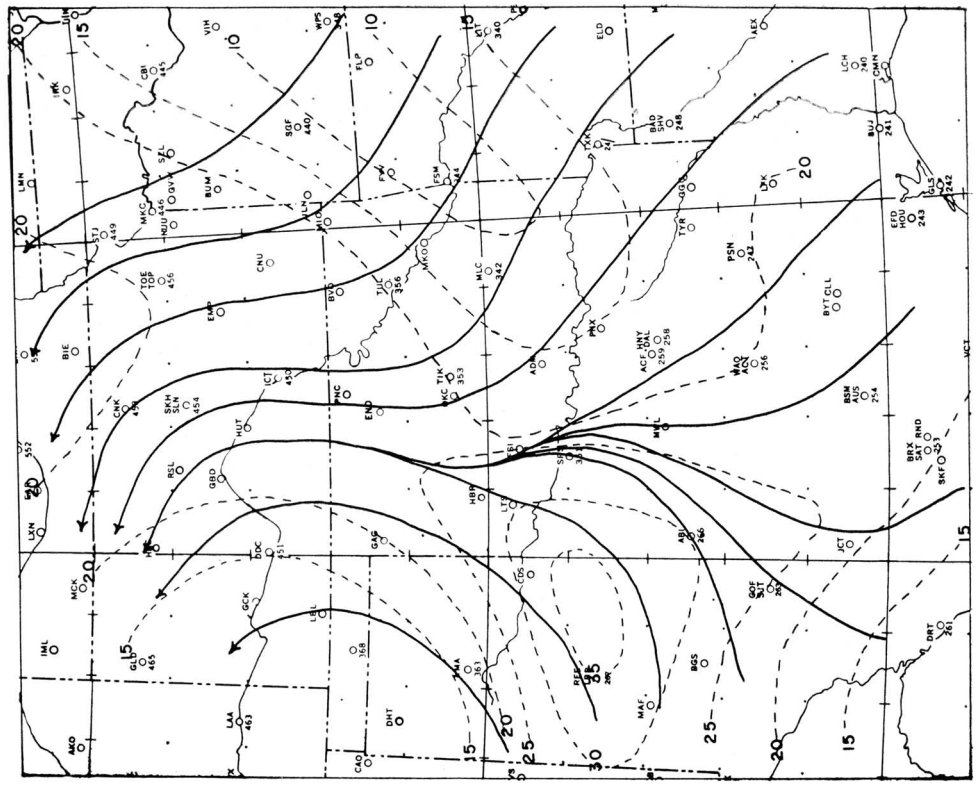

FIG. 4b. 1800C 4 May 1960 streamline and isotach analysis based upon second standard level wind observations.

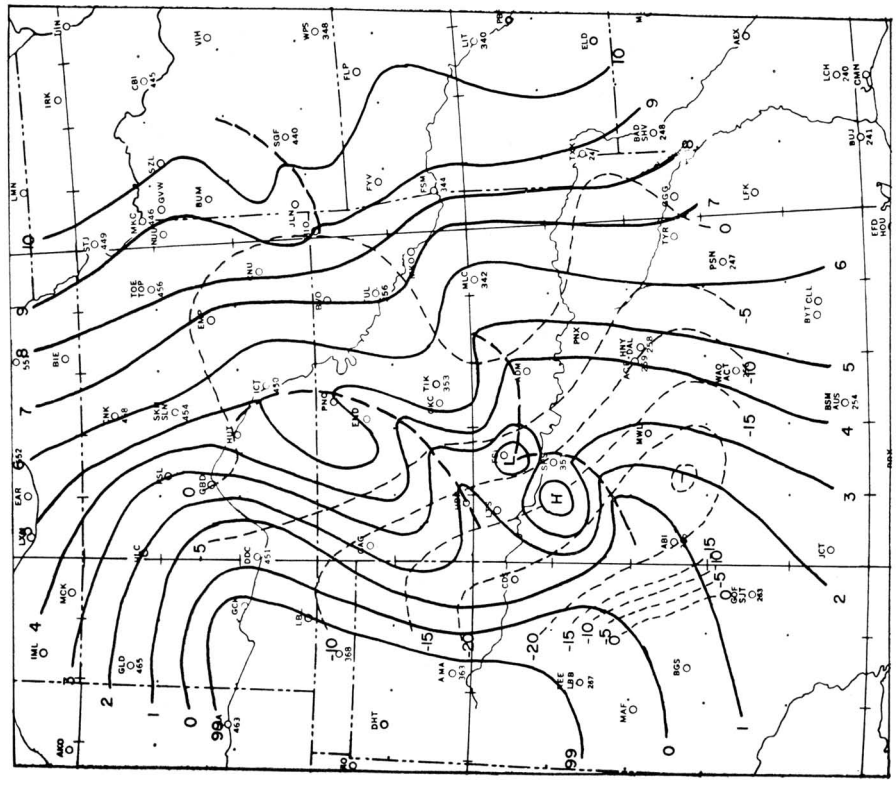

FIG. 4a. 1800C 4 May 1960 surface pressure and horizontal velocity divergence distribution. Solid lines are isobars at one-mb intervals; dashed lines are isopleths of divergence. Units are 10^{-5} hr^{-1}.

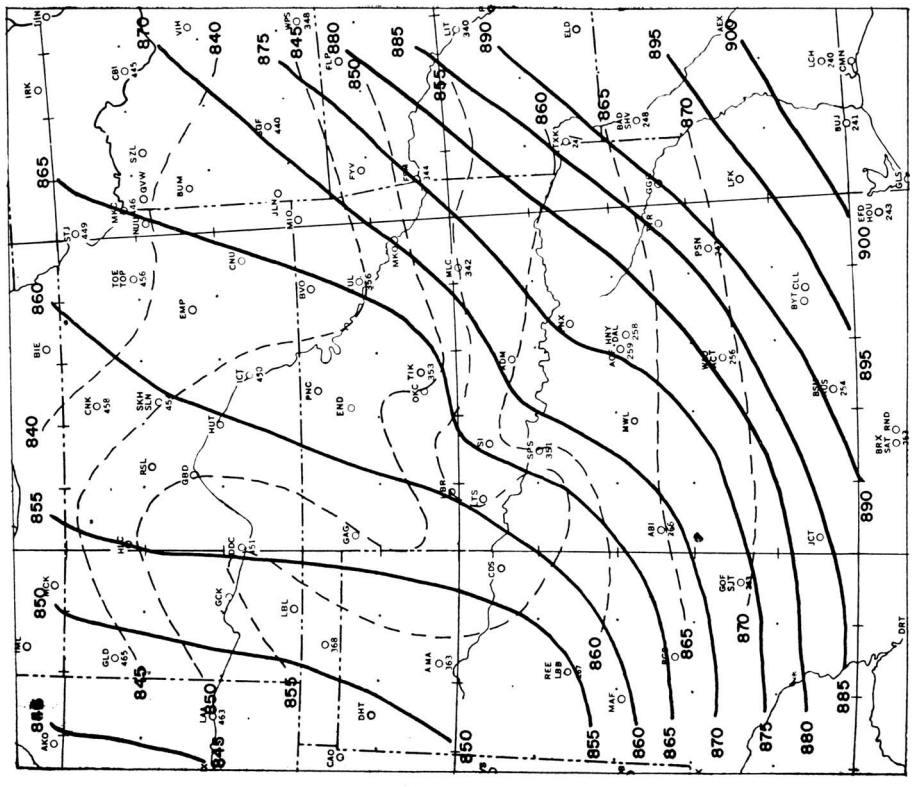

FIG. 4d. 1800C 4 May 1960, 500-mb contours and 1000–500 mb thickness contours. Solid lines are 500-mb contours; dashed lines are thickness contours. All contours are at 50-ft intervals.

FIG. 4c. Isopleths are values of $\partial/\partial t \operatorname{div}_2 V$ at 1800C 4 May 1960. Units are 10^{-2} hr^{-2}.

Fig. 5. Location and times of reported tornado occurrence during period noon to midnight CST 4 May 1960.

Fig. 4e. 1800C 4 May 1960, 200-mb contours and 500-200 mb thickness contours. Solid lines are 200-mb contours at 100-ft intervals; dashed lines are thickness contours at 50-ft intervals.

nostic information that can be readily determined from synoptic surface and upper air data.

Evaluation of the terms in the equations by the forecaster in seeking a solution to a particular forecast problem is of course related to the extent by which the availability of data approaches an optimum with respect to the scale of the phenomena he must predict. The difficulties in this respect are discussed in [6].

Acknowledgment. The efforts of Mr. Clarence L. David of the SELS Forecast Staff who performed the computations, Mrs. Dorothy Babich and Mr. Harry Gordon who drafted the figures and Mrs. Florence Swigert who typed the manuscript are gratefully acknowledged.

REFERENCES

1. U. S. Weather Bureau, 1956: *Forecasting tornadoes and severe thunderstorms,* Forecasting Guide No. 1. Washington, D. C.
2. Fawbush, E. J., R. C. Miller, and L. G. Starrett, 1951: An empirical method of forecasting tornado development. *Bull. Amer. meteor. Soc.,* **32**, 1–9.
3. Lee, J. T., and J. G. Galway, 1956: Preliminary report on the relationship between the jet at the 200-mb level and tornado occurrence. *Bull. Amer. meteor. Soc.,* **37**, 327–332.
4. Magor, B. W., 1959: Meso-Analysis: Some operational analysis techniques utilized in tornado forecasting. *Bull. Amer. meteor. Soc.,* **40**, 499–511.
5. Magor, B. W., 1958: A meso low associated with a severe storm. *Mon. Wea. Rev.,* **86**, 81–90.
6. House, D. C., 1960: Remarks on the optimum spacing of upper air observations. *Mon. Wea. Rev.,* **88**, 97–100.
7. Gilman, C. S., K. R. Peterson, C. W. Cochrane, and S. Malansky, 1960: *On quantitative precipitation forecasting.* NHRP Report No. 38. Washington, D. C.

NEWS AND NOTES

Global Computer Conference Planned

Plans are already underway for United States participation in a second international congress on information processing to be held in Munich on 27 August to 1 September 1962 under sponsorship of the International Federation of Information Processing Societies (IFIPS). The United States member of IFIPS is AFIPS, newly formed from the Joint Computer Committee established ten years ago by the American Institute of Electrical Engineers, the Institute of Radio Engineers, and the Association for Computing Machinery. Dr. E. L. Harder, vice president of the American Institute of Electrical Engineers and manager of the Advanced Systems Engineering and Analytical Department, Westinghouse Electric Corporation, has been appointed chairman of the committee for United States participation.

The IFIP Congress 1962 will resume the activities of the International Conference on Information Processing sponsored by UNESCO in Paris in June, 1959. Through numerous technical sessions and an extensive exhibit of new equipment from all over the world the forthcoming conference is expected to achieve an exchange of information among information technologists of all countries.

Two New Grants for Atmospheric Physics at the University of Nevada

Edgar J. Marston, retired industrialist of La Jolla, California, has donated $150,000 to support a research professorship in atmospheric physics at the University of Nevada's Desert Research Institute. Mr. Marston has been interested in the Desert Research Institute since the idea for its development was first formulated. The fund will be used to endow a faculty chair to be known as the Edgar J. Marston Research Professorship of Atmospheric Physics.

A new grant of $990,000 was made to the Desert Research Institute in September by the Max C. Fleischmann Foundation. The Fleischmann gift will be used to support five professorships, provide new facilities for research and a specialized library collection, and pay administrative expenses for a five-year period.

President Charles J. Armstrong of the University of Nevada described the grants as a "magnificent stimulus to a research program that will reap benefits for the State of Nevada for generations to come." Dr. Armstrong praised the vigorous leadership of the Desert Research Institute by its director, Prof. Wendell A. Mordy, who in less than a year "has shaped the DRI into an important and integral part of the University."

Meeting on Cloud Drop Samplers

A meeting was held during November, 1961, at the Observatoire du Puy de Dome, Clermont, France, under the direction of Henri J. J. Dessens, director of the Observatory. The purpose of the meeting was the experimental comparison of the collection, numbering, and measurement techniques available for cloud and haze droplets. Simultaneous determinations by mechanical, electric, optic, and photoelectric equipment were featured in the study.

(Continued on page 861)